

ARTICLE



SRT1720 inhibits the growth of bladder cancer in organoids and murine models through the SIRT1-HIF axis

Ping Tan ^{1,2}, Manli Wang ^{1,2}, Ailing Zhong¹, Yiyun Wang¹, Jiajia Du¹, Jian Wang¹, Lu Qi¹, Zhanying Bi¹, Peng Zhang¹, Tianhai Lin¹, Jiapeng Zhang¹, Lu Yang¹, Jingyao Chen¹, Ping Han¹, Qiyong Gong ¹, Yu Liu¹, Chong Chen ¹ and Qiang Wei ¹✉

© The Author(s), under exclusive licence to Springer Nature Limited 2021

There are unmet clinical needs for novel therapeutic targets and drugs for bladder cancer. Majority of previous work relied on limited bladder cancer cell lines, which could not well represent the tumor heterogeneity and pathology of this disease. Recently, it has been shown that cancer organoids can recapitulate pathological and molecular properties of bladder cancer. Here, we report, by our knowledge, the first bladder cancer organoid-based small molecule screening for epigenetic drugs. We found that SRT1720, a Sirtuin 1 (SIRT1) activator, significantly inhibits the growth of both mouse and human bladder cancer organoids. And it also restrains the development of mouse *in situ* bladder cancer and human PDX bladder cancer. Mutation of *Sirt1* promotes the growth of cancer organoids and decreases their sensitivity to SRT1720, which validate *Sirt1* as the target of SRT1720 in bladder cancer. Mechanistically, SRT1720 treatment represses the hypoxia pathway through deacetylating HIF1α by activating Sirt1. Genetic or pharmaceutic inhibitions of HIF mimic the anti-tumor effect of SRT1720. Furthermore, the SIRT1-repressed gene signature is associated with the hypoxia target gene signature and poor prognosis in human bladder cancers. Thus, our study demonstrates the power of cancer organoid-based drug discovery and, in principle, identifies SRT1720 as a new treatment for bladder cancer.

Oncogene; <https://doi.org/10.1038/s41388-021-01999-9>

INTRODUCTION

Muscle-invasive bladder cancer (MIBC), consisting of about 20% of newly diagnosed bladder cancer, is an aggressive malignancy with poor prognosis [1, 2]. The current treatments for MIBC are radical cystectomy and systemic chemotherapy, which were first introduced more than 40 years ago. Regimens featuring platinum-based agents (such as gemcitabine and cisplatin) are the backbone of current first-line systemic chemotherapy for patients with advanced-stage bladder cancer. Despite initial objective response in some patients, chemoresistance inevitably develops in nearly all patients and the tolerance of systemic chemotherapy is poor [3]. Thus, new treatments could precisely target tumor cells with fewer side effects desperately needed for MIBC.

Targeted therapy is a type of personalized medical therapy with improved effectiveness and fewer side effects. The first targeted drug, Erdafitinib, was approved for metastatic bladder cancer with FGFR alterations recently [4]. The objective tumor response to Erdafitinib therapy was 40% and the median progression-free survival and overall survival were 5.5 and 13.8 months, respectively [4]. However, it is only applicable to patients with FGFR mutations, which only account for 10–20% of MIBC patients. Therefore, novel therapeutic targets and drugs are in need for those without FGFR alterations.

Efforts have been made to identify therapeutic targets and corresponding drugs for MIBC. However, the majority of these

studies were performed on 2D cultured bladder cancer cell lines. It has been shown that cancer cell lines have alterations in biologic properties, including genetic expression alteration, biological behaviors change, and heterogeneity loss [5]. Thus, these cell line models fail to recapitulate the histopathological features of human disease, and as a result, these studies have poor translational potential. In contrast, recently developed cancer organoids from colorectum, brain, stomach, lungs, liver, and pancreas, as well as bladder can closely mimic the key characteristics of parental tumors including molecular properties, tumor heterogeneity, and most importantly its responses to clinic drugs of the corresponding patient [6–11]. These 3D cultured cancer organoids provide unprecedented opportunities to screen novel drugs. However, bladder cancer organoids from patients showed a large heterogeneity due to individual variation [12, 13]. Genetics-defined cancer organoids can be established from animal models, which could represent the pathological features of this disease with specific mutations. Overall, drivers-defined cancer organoids from model animals are of value to screen novel drugs and yield new therapeutics for the treatment of this disease.

Among the potential target drugs, those involved in epigenetic regulations emerge as new candidates for bladder cancer treatment. It has been shown that 50–90% of bladder tumors contain DNA hypermethylation, and nearly 90% of MIBC have at least one histone modification alteration, including

¹Department of Urology, Institute of Urology, Department of Thoracic Oncology, State Key Laboratory of Biotherapy and Cancer Center, Huaxi MR Research Center (HMRRC), Department of Radiology, West China Hospital, Sichuan University, Chengdu, China. ²These authors contributed equally: Ping Tan, Manli Wang. ✉email: chongchen@scu.edu.cn; weiqiang@scu.edu.cn

histone deacetylases (HDACs), histone acetyltransferases (HATs), histone methyltransferases (HMTs), and histone demethylases (HDMs) [13–16]. These epigenetic modifications play significant roles in gene regulation, DNA repair, cell cycle, and cell invasion, which are involved in tumorigenesis and treatment responses of MIBC [17, 18]. Therefore, it would be interesting to test whether drugs targeting these dysregulated epigenetic factors would be effective to treat MIBC.

In this study, we developed genetic-defined bladder cancer organoids with mutations of *Trp53*, *Rb1*, and *Pten*, and amplification of *Kras^{G12D}* and *c-Myc* from an orthotopic primary bladder cancer mouse model. We performed screening of an epigenetic drug library using mouse bladder cancer organoids. One of the top candidates, SRT1720, a SIRT1 activator [19], was scored and then validated in vitro and in vivo. Furthermore, the potential molecular mechanism of SRT1720 in MIBC was explored by transcriptional analysis.

RESULTS

Organoid-based epigenetics drug screening for MIBC

We established bladder cancer organoids derived from primary orthotopic MIBC mouse models with disruption of *Trp53*, *Rb1*, and *Pten*, and overexpression of *Kras^{G12D}* and *c-Myc*. These mice MIBC organoids represented the features of highly proliferation and expressed the marker of human MIBC, indicated by highly expression of Edu and Cytokeratin 7 (CK7) (Fig. 1A). Furthermore, a platform to identify potential drugs based on these drivers-defined MIBC organoids was established (Fig. 1B).

A total of 276 compounds targeting epigenetic factors, HMTs, HDMs, HATs, DNA methyltransferase, and epigenetic readers [20, 21] (Fig. 1C), were screened on our organoid-based screening platform. The survival of the organoids was measured by Cell Counting Kit-8 (CCK-8) and inhibition scores were calculated by 100% minus the percentages of CCK-8 reads normalized to those treated with vehicle for each molecule (Fig. 1D). All of these drugs were ordered according to their inhibition scores (Fig. 1E). Among the library, 24 molecules inhibited the growth of the MIBC organoids for more than 90% and 50 inhibited for 50–90%. The top candidates included nine HDAC inhibitors, six HMT inhibitors, and two epigenetic reader inhibitors (Fig. 1F). Panobinostat and Chaetocin, inhibitors of HDAC and HMT, respectively, were also scored in our screening (Fig. 1G), which were able to repress the growth of bladder cancer [22, 23].

Identifying SRT1720 as a new inhibitor for MIBC

Among the top candidates, SRT1720, a sirtuin 1 agonist [19], was especially interesting to us (Fig. 1E). Sirtuin 1 has been heavily studied in aging and other human pathological conditions. Its agonists have been reported to be safe and beneficial, at least, for some patients in clinical trials [24–26]. However, the roles of sirtuin 1 and its agonists in cancers are controversial [27]. In the screening, treatment of 10 μM SRT1720 reduced the growth of cancer organoids to 7% of vehicle-treated ones (Fig. 1G).

To validate the library screening, we re-tested the effect of SRT1720 with different concentrations on MIBC organoids. The results showed that SRT1720 inhibited the growth of bladder cancer organoids in a dosage-dependent manner (Fig. 2A) with IC₅₀ of 0.35 μM (Fig. 2B). In contrast to its significant repression on MIBC organoids, SRT1720 presented low cytotoxicity on normal bladder organoids at concentrations between 0.1 and 2.5 μM.

To further test the in vivo therapeutic effect of SRT1720, an orthotopic MIBC mouse model was generated by transplanting the aforementioned MIBC organoids into the bladder of recipient

mice. Five days after transplantation, the mice with similar initial fluorescence signal intensities were signed into two groups treated with vehicle or 40 mg/kg SRT1720, respectively (Fig. 2C). The fluorescence intensities of recipients treated with vehicle increased 60 folds over 9 days, while SRT1720 treatment significantly restrained the tumor growth in vivo (Fig. 2D, E). Consistent with the fluorescence signal intensities, tumors in SRT1720-treated mice were significantly smaller than those in vehicle-treated mice ($p < 0.05$, Fig. 2F–H). H&E showed that there were larger necrotic areas in tumors treated with SRT1720 than those with vehicle (Fig. 2H). Collectively, the data demonstrated that SRT1720 substantially inhibited the growth of MIBC both in vitro and in vivo.

Validating Sirt1 as a therapeutic target for MIBC

SRT1720 had been shown to be an activator of SIRT1 [19] and therefore we wondered whether SRT1720 would repress MIBC through activating SIRT1, a potential new therapeutic target for MIBC. IHC staining showed that SRT1720 treatment increased the expression of SIRT1 in MIBC from mice (Fig. 3A, B). Then, we checked the expression levels of *SIRT1* in human MIBC by analyzing the TCGA cohort [28]. The result showed that the expression levels of *SIRT1* were significantly lower in MIBC than normal bladder tissues (Fig. 3C). We also confirmed the reduced expression of SIRT1 in bladder cancer tissues compared with paired normal urothelial tissues by IHC staining from five patients (Fig. 3D, E).

Next, we tested the roles of SIRT1 by CRISPR/Cas9-mediated mutation in MIBC organoids. Cas9 and sgRNAs targeting *Sirt1* or Scramble sequence were introduced into cancer organoids with lentivirus. The results of blotting revealed that SIRT1 was efficiently disrupted (Fig. 3F). *Sirt1* mutation significantly enhanced the growth of bladder cancer organoids, compared to those with Scramble sgRNA (Fig. 3G, H). This result suggested that SIRT1 might have tumor suppression activity on MIBC.

Then, we went to test whether SIRT1 would be required for the function of SRT1720 on MIBC. We treated the sgScr and sg*Sirt1* MIBC organoids with vehicle or SRT1720. SRT1720 displayed a significant inhibition in the growth of cancer organoids with Scramble sgRNA. In contrast, it had minimal effect on those with *Sirt1* disruption (Fig. 3I, J). Thus, these results strongly suggested that SRT1720 repressed MIBC through SIRT1.

SRT1720 treatment repressed the HIF signaling pathway in MIBC

To explore the molecular mechanisms of SRT1720 on suppressing MIBC tumor, RNA-sequencing was performed to compare the transcriptomics of MIBC organoids treated with SRT1720 or vehicle. The heatmap showed the differentially expressed genes (DEGs) between SRT1720 treatment and vehicle groups. The DEGs showed the pro-survival factors (such as *Eno2*), and oncogenes (including *Irs2* and *Klf7*) were downregulated, while anticancer agents (such as *Tnfsf10*), pro-apoptosis factors (such as *Bcl2l14* and *Dynll1*), and DNA repair-related genes (including *Fancm*, *Faap24*, and *Nudtl*) were upregulated after SRT1720 treatment (Fig. 4A). The KEGG pathway analysis revealed that downregulated genes were significantly enriched in multiple cancer-related pathways after SRT1720 treatment (Fig. 4B). Furthermore, gene set enrichment analyses (GSEA) showed that the HALLMARK_HYPOXIA gene set was one of the most significant negative enriched gene signatures in SRT1720-treated organoids, compared to those with vehicle (NES = -1.56, FDR $q = 0.02$), together with the Epithelial_Mesenchymal_Transition gene set (NES = -1.89, FDR $q = 0.00$) and Angiogenesis gene set (NES = -1.26, FDR $q = 0.16$) (Fig. 4C). Importantly, these pathways were also significantly negative

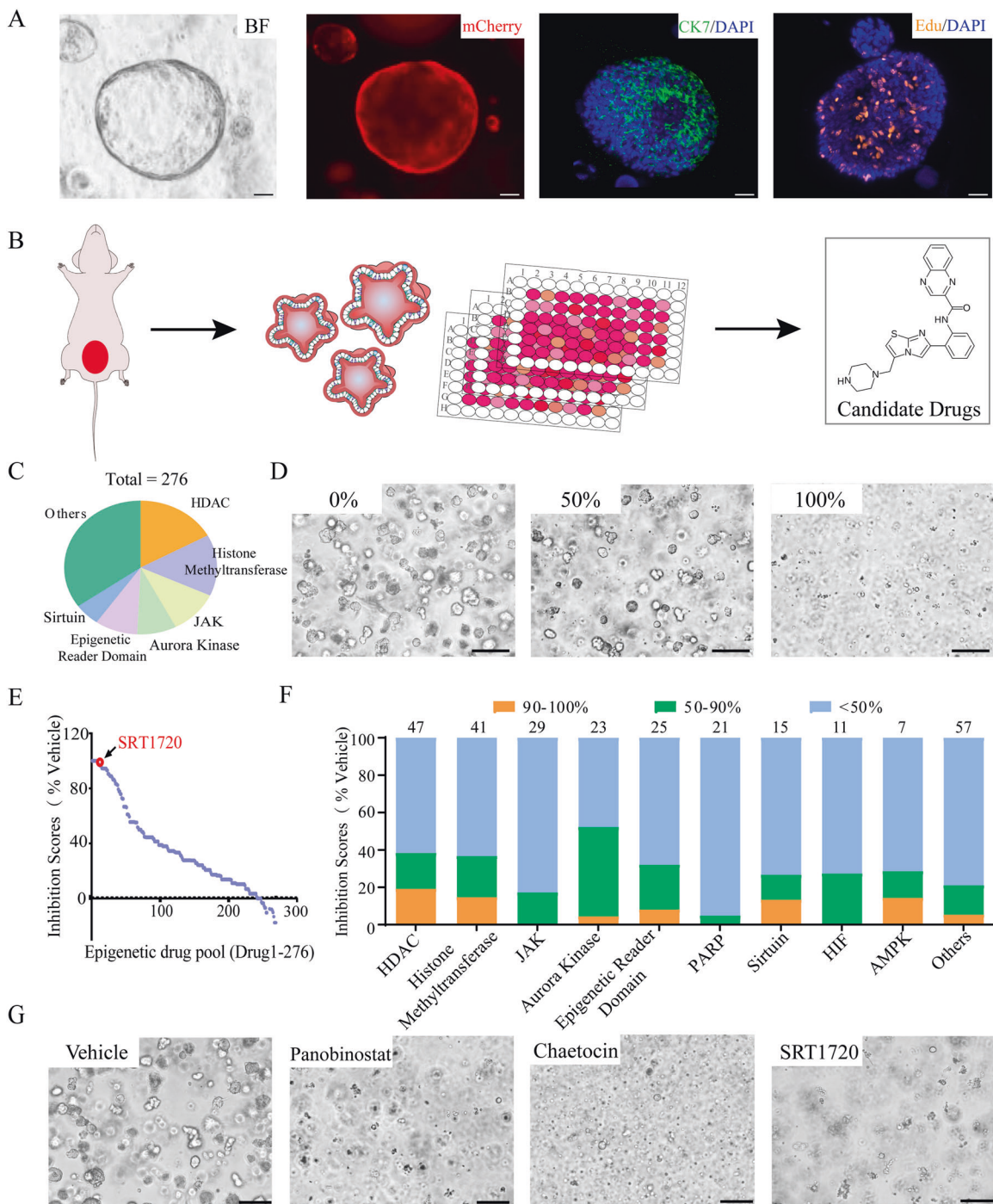


Fig. 1 Organoid-based epigenetics drug library screening identified SRT1720 as a candidate drug for bladder cancer. **A** Representative images and whole-mount Edu (orange) and CK7 (green) staining of mouse bladder tumor organoids after 7 days of culture. Scale bars, 30 μ m. **B** Schematic showing the drug library screening strategy on bladder cancer organoids. **C** Summary of drug classification in the epigenetic drug library. **D** Representative images showing organoids with indicated inhibition scores after drug treatment. Scale bar, 100 μ m. **E** Summary of epigenetics drug library screening, showing the percentages of surviving organoids treated with each drug, comparing to vehicle. **F** Distribution of epigenetics drugs according to their inhibition efficacy of cancer organoids growth. **G** Incidence of different inhibition scores (>90%, 50–90%, <50%) in each kind of target, the numbers above every column are the drug numbers of each target. **H** Representative images showing cancer organoids treated with vehicle, Panobinostat, Chaetocin, and SRT1720 (10 μ M). Scale bars, 100 μ m.

enriched in human MIBC patients with high activity scores of *SIRT1*, compared to those with low activity scores in the TCGA cohort (Fig. 4D).

The repression of the HIF pathway by SRT1720 in MIBC was confirmed by the reduced expression levels of HIF target genes, such

as *Vegfa*, *Jun*, *Pim1*, and *Eno2*, measured by qRT-PCR (Fig. 4E). Furthermore, IHC staining showed that the levels of HIF1 α were decreased in SRT1720-treated MIBC (Fig. 4F, G). These results indicated that SRT1720 treatment repressed the HIF signaling pathway in MIBC.

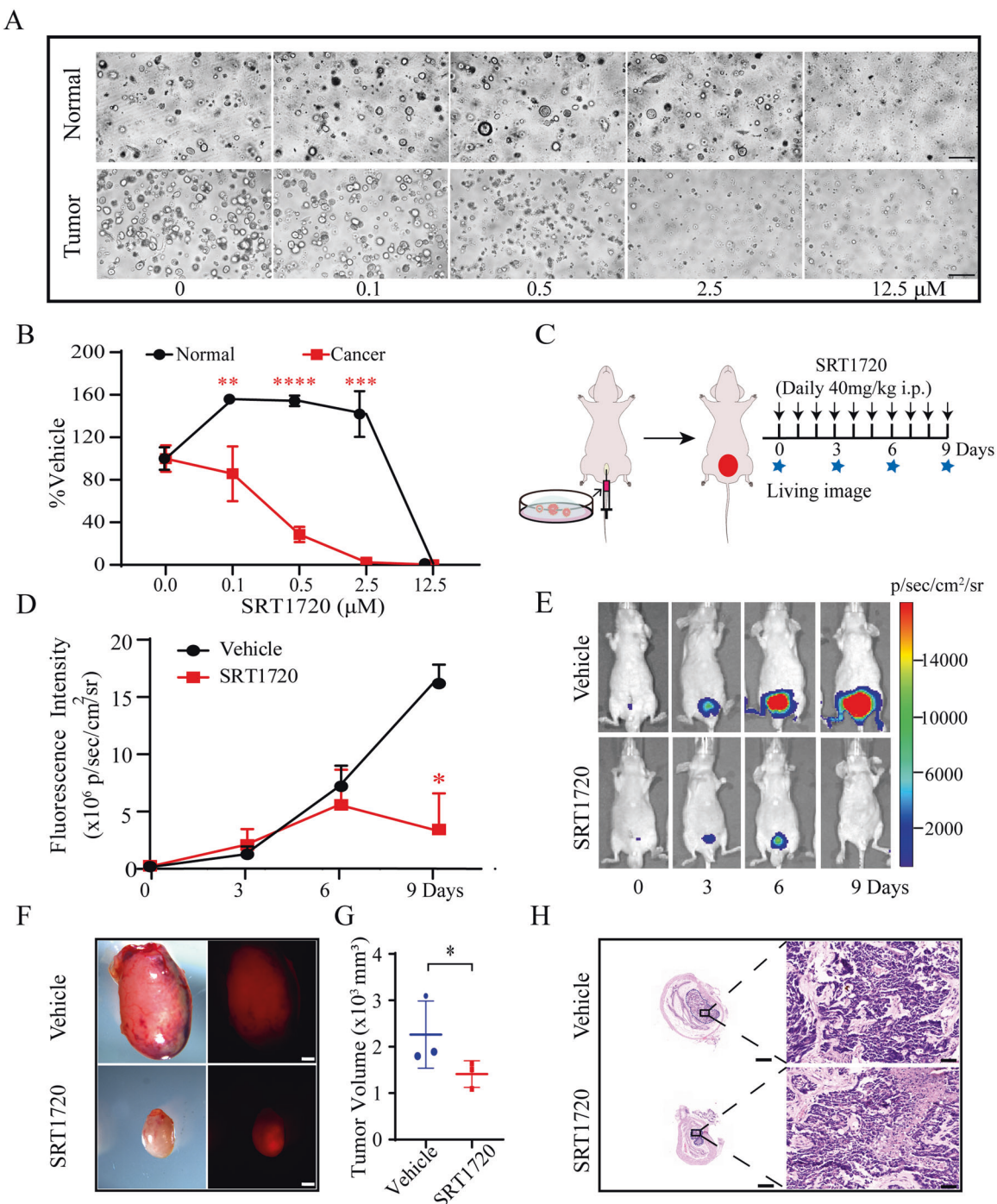


Fig. 2 SRT1720 inhibited the growth of mouse bladder cancer organoids in vitro and organoids-derived orthotopic cancer in vivo.

A Representative images showing mouse normal and cancer bladder organoids treated with vehicle or SRT1720 at indicated concentrations. Scale bars, 200 μm . **B** Survival percentages of normal and cancer organoids treated with SRT1720, comparing to vehicle. ** $p < 0.01$; *** $p < 0.001$; **** $p < 0.0001$. **C** Schematic showing the strategy of SRT1720 treatment in mouse organoids-derived orthotopic bladder cancer. **D** Fluorescence intensity of mice with organoids-derived orthotopic bladder cancer treated with vehicle or SRT1720 over time. $n = 3$; * $p < 0.05$. **E** Representative fluorescence images of mice treated with vehicle or SRT1720 over time. Left, bright field. Right, mCherry. Scale bars, 1 mm. **F** Representative images of bladders from mice treated with vehicle or SRT1720 for 9 days. Left, bright field. Right, mCherry. Scale bars, 1 mm. **G** Tumor volumes in mice treated with vehicle or SRT1720. $n = 3$; * $p < 0.05$. **H** Representative images showing H&E staining of bladder cancer treated with vehicle or SRT1720. Scale bars, left: 1 mm; right: 50 μm .

SRT1720 inhibited the growth of bladder cancer through downregulating the HIF pathway

To evaluate the roles of the HIF pathway in MIBC, we further disrupted *Hif1α* and *Hif1β* in cancer organoids with CRISPR/cas9. Loss of either *Hif1α* or *Hif1β* significantly reduced the numbers of

cancer organoids, compared to those with Scramble sgRNA (Fig. 5A, B). The HIF target genes, including *Vegfa*, *Pim1*, *Ccng2*, *Klh24*, and *Mxi1*, were downregulated in organoids with *Hif1α* or *Hif1β* mutations (Fig. 5C). Together, knockout *Hif1α* reversed the killing effect of SRT1720 on tumor organoids (Fig. 5D, E). Moreover, we

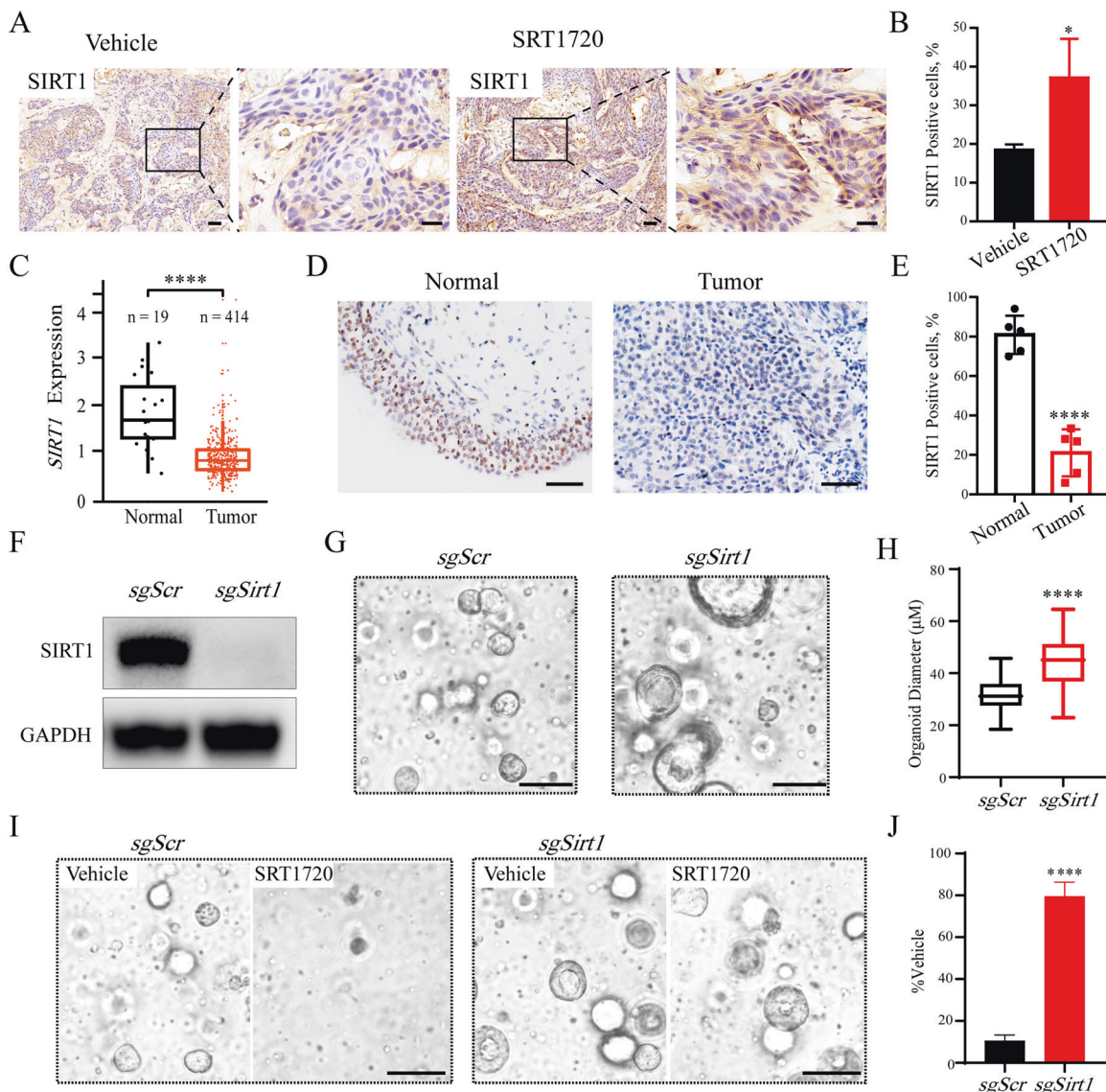


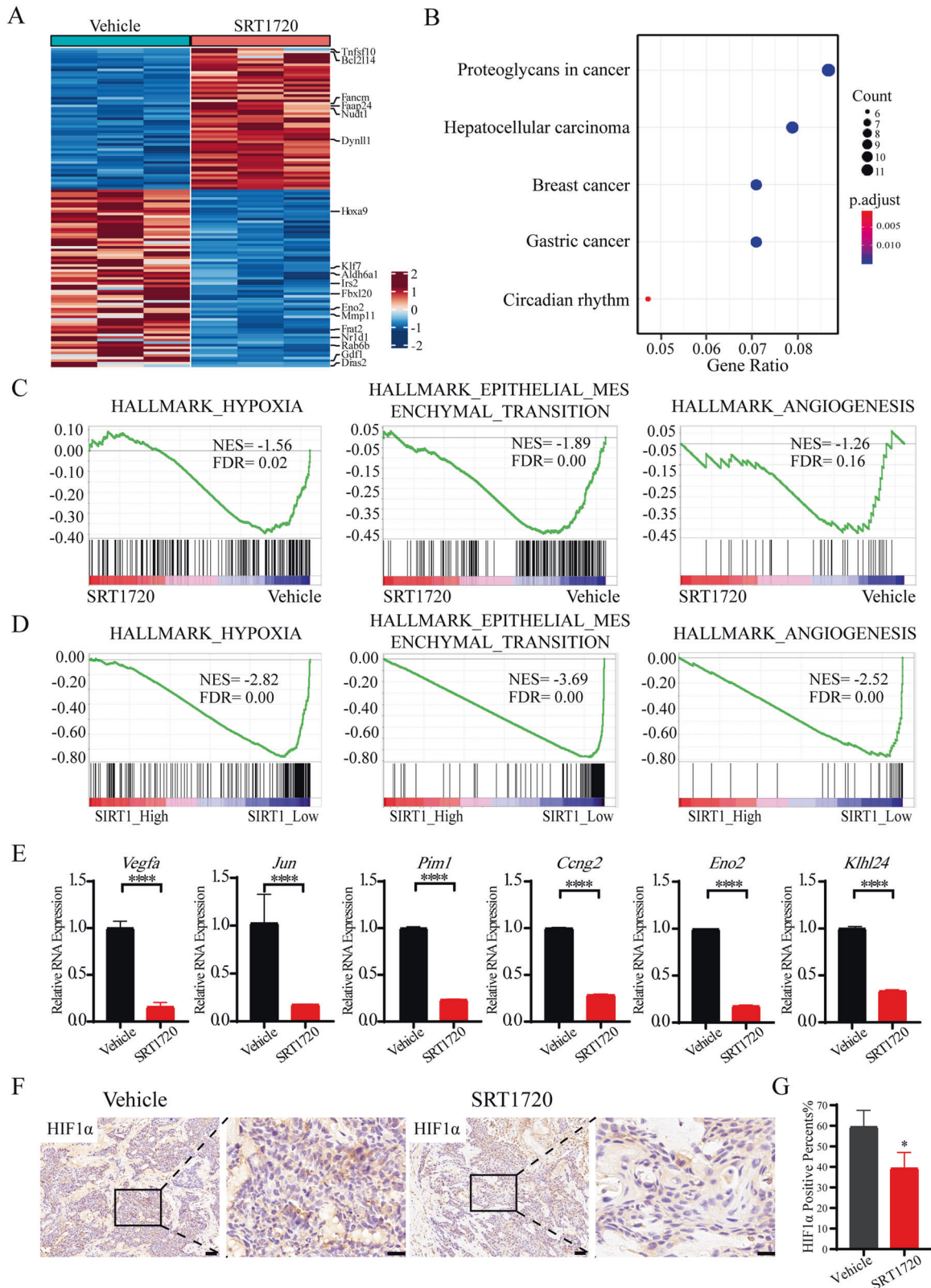
Fig. 3 Validating SIRT1 as the target of SRT1720 in bladder cancer. **A** Representative images showing IHC staining of SIRT1 in bladder cancer tissues from mice treated with vehicle or SRT1720. Left, scale bars, 50 μm; Right, scale bars, 20 μm. **B** Quantification of SIRT1 expression in (A). *p < 0.05. **C** Relative expression levels of SIRT1 in normal bladder tissues and bladder cancer tissues in patients. Data analyzed from TCGA cohorts. ****p < 0.0001. **D** Representative images showing IHC staining of SIRT1 in normal bladder tissue and bladder cancer. Scale bars, 50 μm. **E** Quantification of the expression of SIRT1 protein in paired normal urothelial cells and MIBC tumor cells. n = 5; ****p < 0.0001. **F** Western blotting plots of SIRT1 expression in mouse bladder cancer organoids with or without *Sirt1* knock out. **G** Representative images of bladder cancer organoids with Scramble or *Sirt1* sgRNAs. Scale bar, 100 μm. **H** The size of cancer organoids with Scramble or *Sirt1* sgRNAs. ****p < 0.0001. **I** Representative images showing cancer organoids with Scramble or *Sirt1* sgRNAs treated with 3 μM SRT1720 or vehicle. Scale bar, 100 μm. **J** Survival percentages of cancer organoids with Scramble or *Sirt1* sgRNAs treated with 3 μM SRT1720. **p < 0.01.

checked the HIF target genes expression in mouse bladder cancer organoids with or without *Hif1a* knockout treated with vehicle or SRT1720, we found that the inhibitory effect of SRT1720 on HIF target genes was impaired by *Hif1a* knockout (Fig. 5F, G). These data indicating HIF pathway mediated the activity of SRT1720 in bladder cancer.

As reported, the SIRT1 could deacetylate H3K9ac, H3K14ac, and other targets [29]. Therefore, to evaluate the activity of SIRT1 activated by SRT1720, we first analyzed the level of acetylated histone H3 (Ac-H3) in bladder cancer organoids treated with or without SRT1720. The results suggested that SRT1720 reduced the Ac-H3 level in bladder cancer organoids, indicating the activity of SIRT1 was increased after SRT1720 treatment (Fig. 5H). To acquire an overview of the SIRT1- HIF1α axis, we analyzed the levels of SIRT1 and HIF1α treated by SRT1720 in bladder cancer tissues, and

the results showed the SIRT1 was increased in tumors treated with SRT1720, while HIF1α was decreased (Fig. 5I). However, the mRNA expression level of *Hif1a* was not changed after SRT1720 treatment (Fig. 5J) or *Sirt1* mutation (Fig. 5K) in bladder cancer organoids. Thus, the function of HIF1α may be regulated by SIRT1 at protein level instead of mRNA level.

To further explore their interaction between HIF1α and SIRT1 in bladder cancer, coimmunoprecipitation was performed, and the results suggested that endogenous HIF1α could coprecipitate with SIRT1 in bladder cancer (Fig. 5L). The acetylated HIF1α was also detected by immunoblotting with anti-acetyl lysine in immunoprecipitates by anti-HIF1α in cancer organoids with or without *Sirt1* mutation under normoxia and hypoxia. In our context, we found that the acetylated level of HIF1α was increased after *Sirt1* being disrupted (Fig. 5M); meanwhile, *Sirt1* mutation significantly



enhanced induction of HIF target genes (Fig. 5N). Importantly, after *Sirt1* disruption, we found that the inhibitory effect of SRT1720 on HIF pathway was impaired (Fig. 5O). These results indicated that SIRT1 could bind to and deacetylate HIF1 α , and negatively regulate

the transcriptional activity of HIF1 α in bladder cancer; meanwhile, this negative regulation of SRT1720 on HIF pathway was SIRT1 dependent. Treatment with 2-Methoxyestradiol (2-MeOE2, 5–40 μ M), a HIF1 α inhibitor, resulted in a dose-dependent inhibition

Fig. 4 SRT1720 repressed the HIF pathway in bladder cancer. A Heatmap of differentially expressed genes (DEG) detected between mouse bladder cancer organoids treated with vehicle or SRT1720 for 12 h, measured by RNA-seq. *p* adjust value <0.05. **B** Dot plot showing the most downregulated KEGG pathways enriched in the bladder cancer organoids treated with SRT1720, comparing to those with vehicle. **C** Gene set enrichment analysis (GSEA) showing the negative enrichment of the Hypoxia, Epithelial-Mesenchymal Transition, and Angiogenesis gene signatures in SRT1720-treated bladder cancer organoids, comparing to those treated with vehicle. **D** GSEA showing the negative enrichment of the Hypoxia, Epithelial-Mesenchymal Transition, and Angiogenesis gene signatures in bladder cancer patients with high expression levels of *SIRT1*, comparing to those with low expression levels of *SIRT1*. Data analyzed from the TCGA cohort. **E** The relative expression levels of *Vegfa*, *Jun*, *Pim1*, *Ccng2*, *Eno2*, and *K1h124* in bladder cancer organoids treated with vehicle or SRT1720, measured by qRT-PCR. $n = 3$; * $p < 0.05$; ** $p < 0.01$; *** $p < 0.001$. **F** Representative images showing IHC staining of HIF1 α in bladder cancer tissues from mice treated with vehicle or SRT1720. Left, scale bars, 50 μ m; right, scale bars, 20 μ m. **G** Quantification of HIF1 α expression in (F). * $p < 0.05$.

of MIBC organoids, which further suggested that the downregulation of HIF pathway played a vital role in SRT1720 treatment in MIBC (Fig. 5P).

SRT1720 suppressed patient-derived organoids and xenografts from human MIBC

Then the suppression activity of SRT1720 in human MIBC was further evaluated. Cancer organoids were established from three MIBC patients who underwent radical cystectomy (Fig. 6A). Similar to mouse MIBC organoids, human cancer organoids represented the histopathological characteristics of human disease, indicated by H&E staining and IHC staining with CK5 and CK7, the common markers of urothelial carcinoma in human. We found that all of these three human MIBC organoid lines responded to SRT1720 treatment in a dosage-dependent manner with IC₅₀ around 2.5 μ M (Fig. 6B, C).

The anti-tumor effect of SRT1720 was further evaluated in vivo in PDX from three MIBC patients. SRT1720 (40 mg/kg) or vehicle was administered through daily intraperitoneal injection for 2 weeks (Fig. 6D). SRT1720 treatment significantly repressed the growth of all three PDX lines, compared to vehicle treatment. And indeed, PDX tumors completely hindered their growth or even shrank after SRT1720 treatment (Fig. 6E–L). Thus, SRT1720 could also repress human MIBC in vitro and in vivo.

Validating the SIRT1-HIF axis in human MIBC

Given the importance of the SIRT1-HIF axis in SRT1720-treated mouse MIBC, we measured the expression levels of SIRT1 and HIF1 α in human MIBC by IHC staining. Consistent with mice bladder tumor, the results showed that SRT1720 treatment significantly enhanced the expression of SIRT1 in human MIBC PDX tumors, while suppressed the HIF1 α expression (Fig. 7A–D). In addition, angiogenesis was also impaired by SRT1720 treatment in bladder cancer PDX tumors validated by CD31 staining (Fig. 7E).

Furthermore, we explored the correlation between SIRT1 and hypoxia pathway in human MIBC. Low SIRT1 activity scores, defined by the expression levels of the SIRT1 target genes, were associated with poor prognosis ($p < 0.0001$) in bladder cancer patients from TCGA database (Fig. 7F). In contrast, high hypoxia scores, defined by the expression levels of the hypoxia pathway genes, were associated with poor prognosis ($p < 0.0001$) (Fig. 7G).

It has been reported that SIRT1-mediated TP53 deacetylation is critical for the inhibitory effect of SIRT1-activating compounds (STACs) in several types of cancer cells [27, 30]. To test whether TP53 would be involved in the SIRT1-HIF1 α axis in bladder cancer, we analyzed the correlation of the SIRT1 activity and the prognosis in patients with intact or mutant *TP53*. The results showed that in both groups, low SIRT1 activity was significantly associated with poor prognosis (Fig. 7H, I). These results suggested that the effect of SIRT1 in bladder cancer might be *TP53* independent. More importantly, the SIRT1 expression level and its activity scores were negatively correlated with the hypoxia pathway scores in TCGA bladder cancer cohort ($R = -0.33$, $p < 1.8e-11$, and $R = -0.33$, $p < 1.8e-11$, respectively) (Fig. 7J, K) and MSKCC bladder cancer cohort ($R = -0.53$, $p < 1.9e-5$) (Fig. 7L); and this negative correlation was also *TP53* independent (Fig. 7M, N). Moreover, *SIRT1* mutation significantly enhanced induction of hypoxia associated

genes in bladder cancer patients, showing by volcano map (Fig. 7O). Thus, the SIRT1-HIF1 α axis, which could be disrupted by SRT1720, played an important role in human MIBC.

DISCUSSION

In this work, we have established a platform with mouse and human bladder cancer organoids and their derived in vivo models for drug screening and validation. Although tumor organoids have been suggested for translational studies [9], few studies have successfully applied them for drug screening and mechanism studies for bladder cancer. And their derived in vivo orthotopic models are even more challenging. To our knowledge, this study is one of the first few to fully use all of these organoids and their derived in vivo models for translational studies in bladder cancer. As reported, numerous epigenetic alterations have been identified in bladder cancer, but until now, only five clinical trials evaluating the effect of epigenetic drugs, including HDACs inhibitors and DNA methyltransferase inhibitors, on bladder cancer are ongoing [31, 32]. Thus, based on this drug-screening platform, an epigenetic drug library containing 276 drugs was screened in this study. Besides other already known epigenetic drugs, an unexpected activator SRT1720 was also identified for bladder cancer treatment and it has never been studied in bladder cancer.

SIRT1 was previously proved to improve healthspan and lifespan, suppress inflammation, and regulate aging and metabolic-related diseases [19, 33]. However, the roles of SIRT1 in cancers, as a tumor suppressor or tumor promoter, remain unclear [27]. Meanwhile, the substrates of SIRT1 are proved to differ from one organ to another [34]. Thus, SIRT1 may act differently in different tumors or tissues. Several studies suggested a tumor suppressor role of SIRT1 in breast cancer, multiple myeloma, pancreatic cancer, and colorectal cancer through regulating lysosomal-dependent necrosis, apoptosis, reactive oxygen species, angiogenesis, or wnt signaling pathway [35]. Two recent studies have shown that SIRT1 may promote bladder cancer progression in bladder cancer cell lines through FOXO3a-mediated pathways or by regulating GLUT1 [36, 37]. But in our study, we found that SRT1720, a SIRT1 activator, presented an excellent anti-tumor activity in vitro and in vivo. These paradoxical results might be at least partially attributed to their models, in most of cases, cell lines. Here, we used multiple cutting-edge MIBC models, which represent human diseases precisely, to identify and validate SRT1720 as an effective treatment for bladder cancer. In our screening, we also found that other SIRT1 activators, such as SRT3025, SRT2183, and SRT2104, were able to inhibit bladder cancer organoids, while SIRT1 inhibitors, including Sirtinol and EX527, significantly promoted bladder cancer growth (data not shown). Meanwhile, the bioinformatics analysis found that the SIRT1 activity score positively related to the prognosis in bladder cancer patients. Thus, SIRT1 was more likely to serve as a tumor suppressor instead of a tumor promoter in our context.

SRT1720 is a well-studied second-generation STAC, which has been shown to have excellent pharmacokinetics for better in vivo activation than other STACs [19]. In our library, SRT1720 had the best inhibition effect on bladder cancer organoids during our screening, although several other STACs also showed significant anti-tumor effect. There are some third-generation STACs available at present, such as STAC-5, -9, -10, which might have better performance,

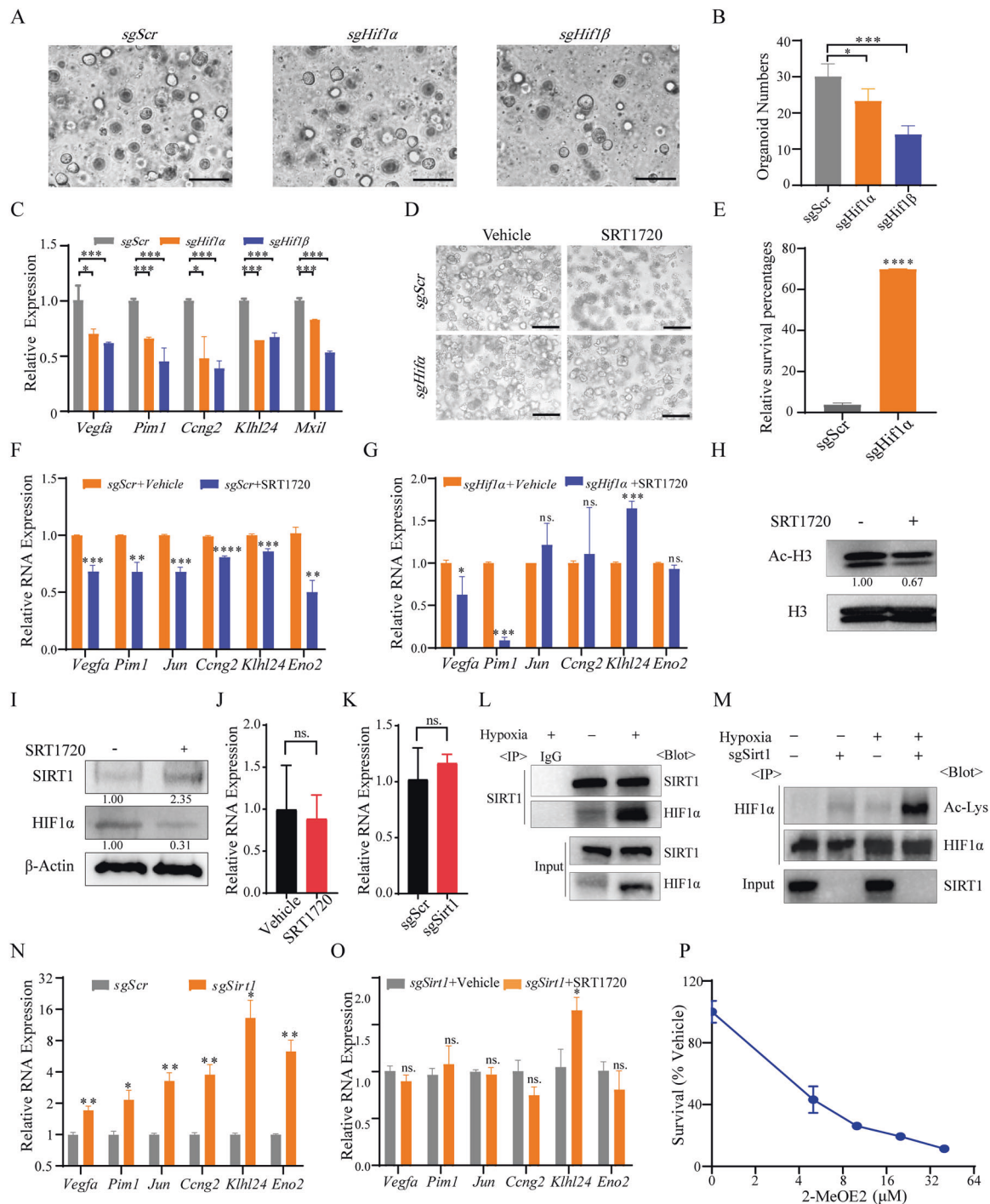


Fig. 5 SRT1720 inhibited the growth of bladder cancer through downregulating the HIF pathway. **A** Representative images of cancer organoids with Scramble, *Hif1α* or *Hif1β* sgRNAs. Scale bars, 200 μm. **B** Numbers of cancer organoids with Scramble, *Hif1α* or *Hif1β* sgRNAs. *p < 0.05; ***p < 0.001. **C** Relative expression levels of HIF target genes (*Vegfa*, *Pim1*, *Ccng2*, *Klh24*, and *Mxil*) in cancer organoids with Scramble, *Hif1α* or *Hif1β* sgRNAs. *p < 0.05; **p < 0.01; ***p < 0.001. **D** Representative images of cancer organoids with Scramble or *Hif1α* sgRNA treated by vehicle or SRT1720 (10 μM). **E** Quantification of survival percentages of cancer organoids in (D). ***p < 0.001. **F**, **G** Relative expression levels of HIF target genes in cancer organoids with Scramble (**F**) or *Hif1α* sgRNA (**G**) treated by vehicle or SRT1720 (10 μM). *p < 0.05; **p < 0.01; ***p < 0.001; ****p < 0.0001. **H** Western blotting plots of histone H3 and acetylated histone H3 (Ac-H3) in mouse bladder cancer organoids treated with vehicle or SRT1720 (10 μM) for 36 h. **I** Western blotting plots of SIRT1 and HIF1α in tumor tissues from primary orthotopic bladder cancer model treated with vehicle or SRT1720 (40 mg/kg/d, i.p.) for 4 days. **J** Relative expression levels of *Hif1α* in cancer organoids with or without SRT1720 treatment. **K** Relative expression levels of *Hif1α* in cancer organoids with Scramble or *Sirt1* sgRNAs. **L** Coprecipitation of endogenous SIRT1 and HIF1α was performed using anti-SIRT1 in mouse bladder cancer organoids incubated under normoxic or hypoxic conditions for 6 h. **M** Endogenous HIF1α was immunoprecipitated with anti-HIF1α, and acetylated HIF1α was identified using anti-acetyl-lysine in mouse bladder cancer organoids with or without *Sirt1* knockout under normoxic or hypoxic conditions for 6 h. **N** Relative expression levels of HIF target genes in cancer organoids with *Sirt1* sgRNA treated with vehicle or SRT1720. *p < 0.05; **p < 0.01. **O** Relative expression levels of HIF target genes in cancer organoids with *Sirt1* sgRNA treated with vehicle or SRT1720. *p < 0.05; ns, not significant. **P** Survival percentages of cancer organoids treated with vehicle or 2-MeOE2.

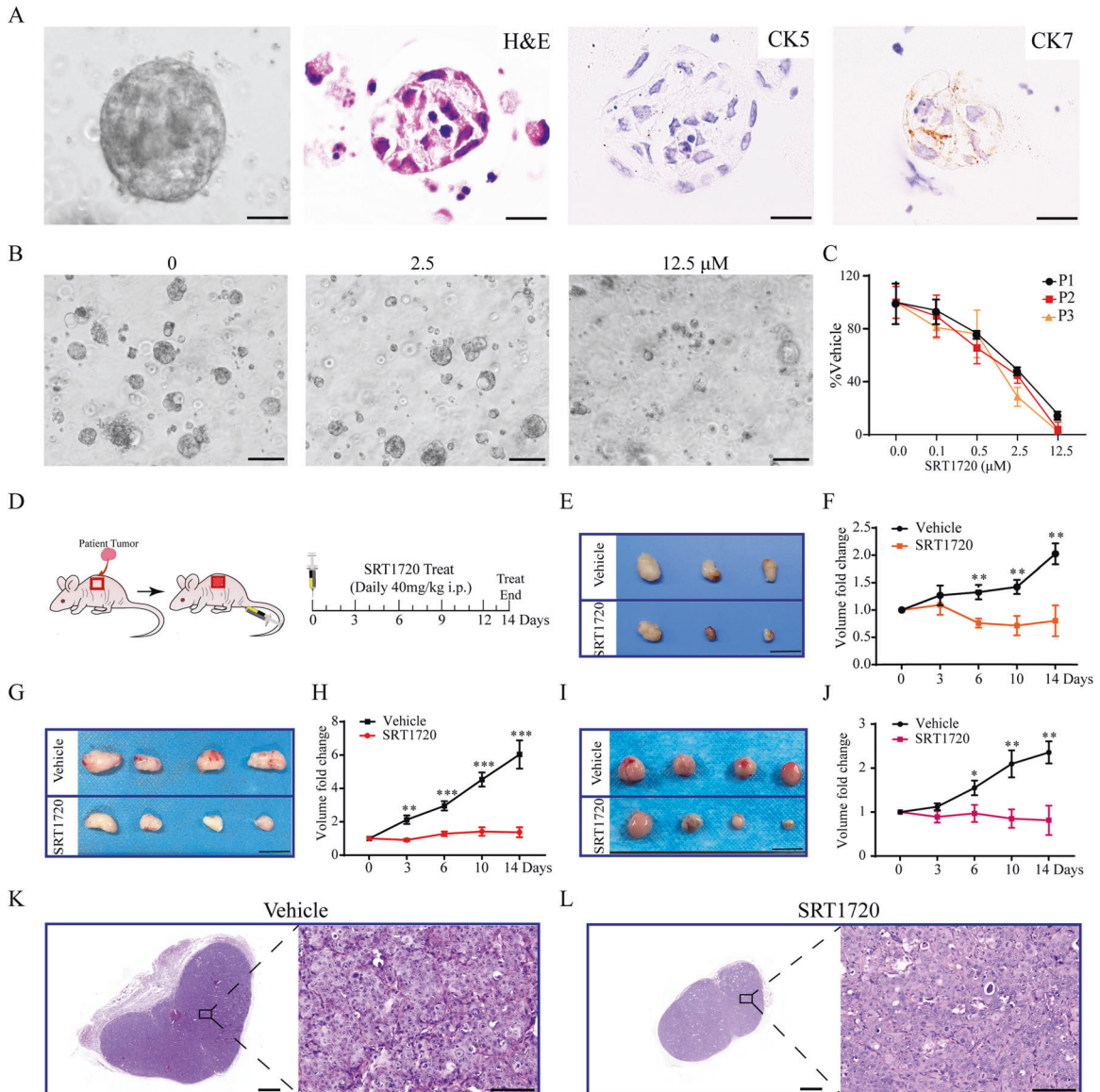


Fig. 6 SRT1720 inhibited the growth of bladder cancer in patient-derived organoids and xenografts. A Representative pictures of human bladder cancer organoids, showing bright-field image, H&E and IHC staining of CK5 and CK7. Scale bars, 50 μm . **B** Representative images showing human bladder cancer organoids treated with vehicle or SRT1720 at indicated concentrations. Scale bars, 100 μm . **C** Survival percentages of human bladder cancer organoids treated with SRT1720, comparing to vehicle, in patient P1, P2, P3. **D** Schematic showing the strategy of SRT1720 treatment in patient-derived xenografts. **E–J** Representative images of bladder cancers treated with vehicle or SRT1720 in PDX models from Patient-1 (**E**), Patient-2 (**G**), and Patient-3 (**I**) and summary of tumor volumes (**F**, Patient-1; **H**, Patient-2; and **J**, Patient-3) over time. * $p < 0.05$; ** $p < 0.01$; *** $p < 0.001$. Scale bars, 10 mm. **K**, **L** Representative images showing H&E staining of human bladder cancer PDX models treated with vehicle (**K**) or SRT1720 (**L**). Scale bars, 1 mm (left) and 100 μm (right).

especially with less toxicity [35]. Unfortunately, our library did not include enough third-generation STACs to test this hypothesis. It would be of interest to evaluate them in future studies.

With multi-omics analyses, CRISPR/Cas9 genome editing, biochemical, and pharmaceutical studies, our results found that SRT1720 suppressed the MIBC growth through regulating SIRT1-HIF1 α axis. Actually, until now, several studies had focused on the interaction between SIRT1 and HIF1 α , but the effect of SIRT1 on HIF1 α transcriptional activity is still under debate [38–41]. Laemmle et al. [40] and Joo et al. [41] reported that there was a positive regulation impact on HIF1 α activity via deacetylation, while others reported that SIRT1 had either no impact [38] or negatively regulated HIF1 α activity [39, 42]. Therefore, it is possible that SIRT1 exerts a dual regulatory function and performs not equally in different tissues. In addition, study reported that SIRT1

could activate HIF2 α , which also drives VEGF expression, such as HIF1 α [43]. However, in this study, we found that the hypoxia pathway and angiogenesis pathway were both downregulated after SRT1720 treatment, as well as VEGF-A expression. Thus, under our context, HIF2 α may not serve as a critical one in killing bladder cancer, and its roles remains to be studied. The effect of hypoxia on SIRT1 expression is still under debate at present. Chen et al. suggested that hypoxia increased SIRT1 expression in liver cancer [44], while Lim et al. claimed that SIRT1 activity also appears to be reduced by hypoxia due to reduced transcription of SIRT1 mRNA and a decrease in the NAD $^+$ /NADH ratio [39].

In terms of HIF1 α protein stability, the evidence has shown that the lysine acetylation regulates protein stability and function. Geng et al. reported that the HIF1 α protein stability is increased by acetylation at lysine 709 [45], while Joo et al. showed that SIRT1 stabilizes HIF1 α by

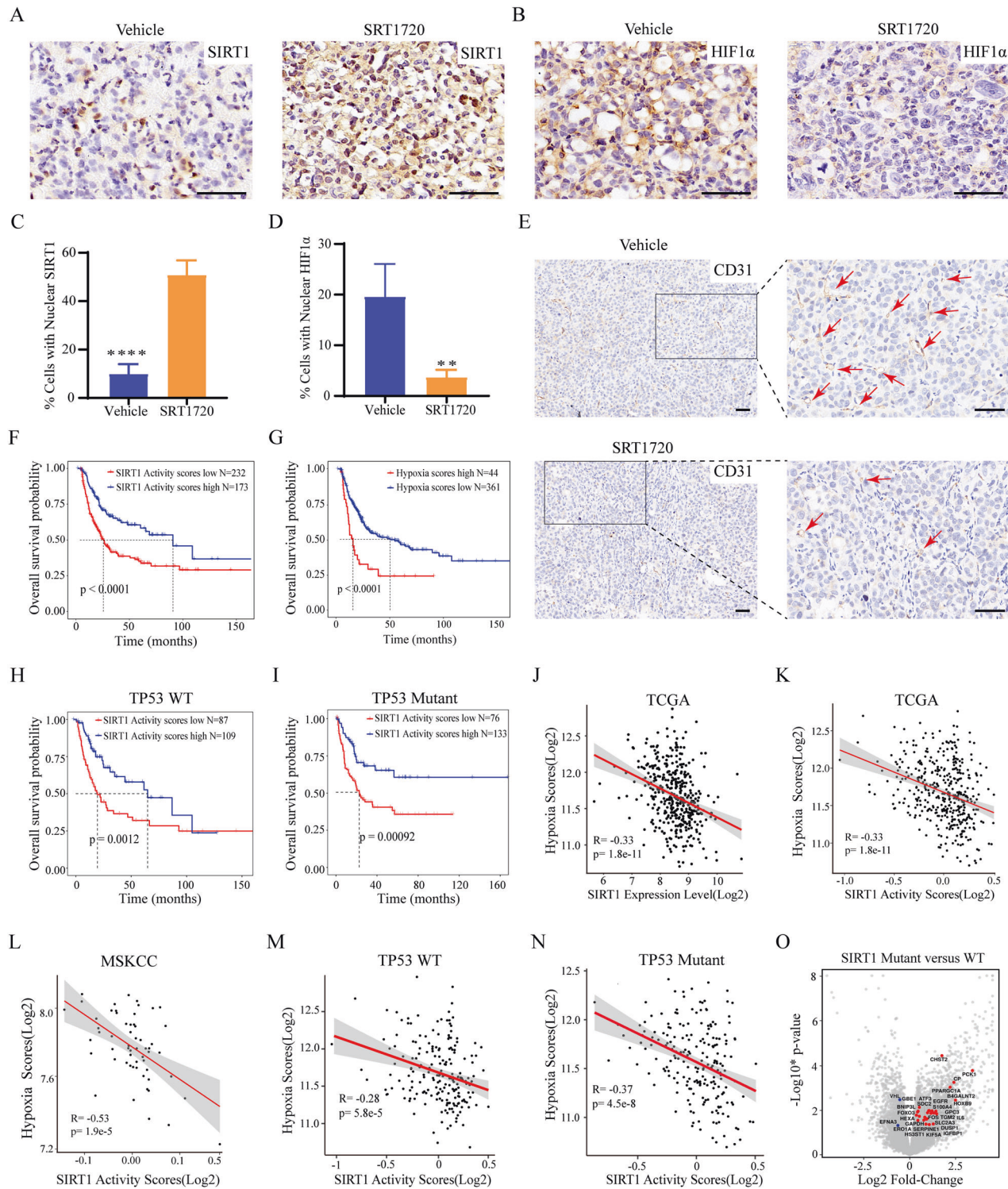


Fig. 7 SRT1720 downregulated the hypoxia pathway through activating SIRT1 to inhibit the growth of human bladder cancer. A–D Representative images showing IHC staining of SIRT1 (A) and HIF1 α (B) and their percentages (C and D) of positive staining cells in bladder cancer PDX models treated with vehicle or SRT1720. Scale bars, 50 μ m. **p < 0.01; ***p < 0.0001. **E** Representative images showing IHC staining of CD31 in PDX tumors treated with vehicle or SRT1720. Red arrows indicate the blood vessels. Scale bars, 50 μ m. **F, G** Kaplan–Meier plots showing the impact of SIRT1 activity (F) and hypoxia scores (G) on the overall survival of bladder cancer patients. Data analyzed from TCGA-BLCA database. **H, I** The Kaplan–Meier survival curves of TCGA-BLCA patients with low or high SIRT1 activity scores in TP53 wild-type (H) and mutant groups (I). **J** The scatter plot showing the correlation between SIRT1 expression level and hypoxia scores in TCGA-BLCA. **K, L** The scatter plots showing the correlation between SIRT1 activity scores and hypoxia pathways scores in TCGA-BLCA (K) and MSKCC-solit-2012 (L) cohorts. **M, N** The scatter plots showing the correlation between SIRT1 activity scores and hypoxia scores in TP53 wild-type (M) and mutant patients (N). **O** Volcano map showing hypoxia associated genes significantly highly expressed or downregulated in bladder cancer patients with SIRT1 mutation. Data analyzed from TCGA-BLCA database. Red dots represent upregulated genes; blue dots represent downregulated genes.

deacetylation [41]. Therefore, the main points of contention are which one, acetylated or deacetylated HIF1 α , has higher stability or transcriptional activity. In this study, we found that SIRT1 could also bind to and deacetylate HIF1 α , and negatively regulate the HIF target genes. In addition, SIRT1 was found to associate with HIF1 α in bladder cancer tissues and regulate tumor growth negatively by using SRT1720. Thus, we are more likely to propose that the activity of HIF1 α is decreased by deacetylation in bladder cancer.

Although SRT1720 was originally revealed to enhance SIRT1 enzymatic activities [19], our study and several other studies also found that SRT1720 treatment could increase the expression level of SIRT1 [46]. Limited evidence suggested that SIRT1 expression could be positively regulated by STACs through a FOXO1-mediated mechanism. By activating SIRT1, SRT1720 can deacetylate and increase the DNA-binding ability of FOXO1, which could further promote the SIRT1 transcription through binding to the SIRT1 promoter region at IRS-1 and FKHD-like responsive elements [46]. Thus, the expression of SIRT1 increased by SRT1720 treatment may be partly attributed to this autofeedback loop mechanism.

SIRT1 is a multifaceted gene and has been involved in regulating various downstream targets and pathways under different contexts. For example, previous study showed that SRT1720 repressed myelodysplastic syndrome stem and progenitor cells by upregulating TET2 function [47]. Chini et al. showed that SRT1720 inhibited pancreatic cancer cell growth through lysosomal-dependent pathway [48]. Wang et al. showed that SIRT1 negatively regulated the mTOR signaling pathway, which, in turn, activated HIF1 α [49]. Of note, TP53 deacetylation by SIRT1 has been proposed to be a critical mechanism for STACs, including SRT1720, on cancers [30]. Interestingly, we found that the prognosis value of SIRT1 activity in bladder cancer patients was independent of TP53 mutation status. Furthermore, in either bladder cancers with or without TP53 mutations, the SIRT1 activity was significantly negatively correlated with the HIF activity. These results strongly agree a non-essential role of TP53 in the repression of SRT1720 on bladder cancer. Instead, with multiple in vitro and in vivo mouse and human MIBC models, we showed that SRT1720 inhibited MIBC through activating SIRT1, which, in turn, deacetylated HIF1 α and repressed the hypoxia pathway. Thus, our study clarified the SIRT1-HIF1 α axis in bladder cancer.

The research strategy of the present study opens the possibility to screen the novel drugs on bladder cancer organoids in vitro and verify their efficacy in patients-derived cancer organoids and PDX models of MIBC in vivo, potentially yielding new therapeutics for the treatment of this disease. Notably, the current findings in our research support that targeting SIRT1 with pharmacological activators such as SRT1720 may be a novel treatment for MIBC.

CONCLUSION

In summary, our study demonstrated the feasibility of cancer organoid-based drug discovery and, in principle, identified SRT1720 as a new treatment for MIBC through regulating the SIRT1-HIF1 α axis.

MATERIALS AND METHODS

Human tumor samples and PDX model generation

All patients had a confirmed pathologic diagnosis of MIBC and underwent radical cystectomy at West China Hospital, Sichuan University. Their tumor tissues were collected immediately after surgery, and then were minced into pieces and injected to NSG mice (male, 6- to 8-week-old) via subcutaneous transplantation.

Orthotopic bladder cancer mouse model establishment

All experiments based on mouse were approved by the institutional Animal Care and Use Committees of Sichuan University. Mouse orthotopic MIBC model was generated by injecting cancer organoids with *Trp53*, *Pten*, and *Rb1* mutations and *c-Myc* and *Kras*^{G12D} amplification into the bladder

of nude Balb/c mice (male, 6- to 8-week-old). The MIBC organoids were established previously in our lab.

Organoids-based drug screening

Mouse bladder cancer organoids were seeded into 96-well plates and cultured for 24 h. The cells were treated with compounds (10 μ M) for 3 days. The cell viability of organoids was quantified using CCK-8 [50]. Inhibition scores of every compound were calculated by normalizing to control group. The selected candidates were further validated.

Gene editing

sgRNA oligos were cloned into the vector pLentiCRISPR V2 plasmid. sgRNA oligo sequences are listed in Supplementary Table 1. The cultured organoids were disassociated using TrypLE. The cells were resuspended with lentiviral supernatants and centrifuged for 1 h followed by another 2 h incubating.

In vivo treatment

For orthotopic bladder cancer mouse models, treatment was initiated 4 days after transplantation. Mice bearing tumors were daily treated with either vehicle or 40 mg/kg SRT1720 (Selleck, S1129) by intraperitoneal injection for 9 days [51]. Tumor volumes were measured every 3 days by using Bioluminescence Imaging. For PDX models, the treatment was started when tumor volumes reached approximately 100 mm³ for 14 days and the tumor volumes were measured every 3 days.

Statistical analysis

The statistical data are presented as mean with standard deviation from three independent experiments. To determine statistical probabilities, unpaired Student's *t* tests or one-way ANOVA was conducted where appropriate. Statistical analysis was performed with GraphPad Prism 7.0. *p* value <0.05 was considered statistically significant difference.

DATA AVAILABILITY

All bulk RNA data generated by this study have been deposited in the GEO data sets (<https://www.ncbi.nlm.nih.gov/gds>). The data can be accessed under the accession number GSE155525. The code is available from the authors on request.

REFERENCES

- Bray F, Ferlay J, Soerjomataram I, Siegel RL, Torre LA, Jemal A. Global cancer statistics 2018: GLOBOCAN estimates of incidence and mortality worldwide for 36 cancers in 185 countries. *CA Cancer J Clin.* 2018;68:394–424.
- Berdik C. Unlocking bladder cancer. *Nature.* 2017;551:S34–S35.
- Vlachostergios PJ, Faltas BM. Treatment resistance in urothelial carcinoma: an evolutionary perspective. *Nat Rev Clin Oncol.* 2018;15:495–509.
- Loriot Y, Necchi A, Park SH, Garcia-Donas J, Huddart R, Burgess E, et al. Erdafitinib in locally advanced or metastatic urothelial carcinoma. *N Engl J Med.* 2019;381:338–48.
- Gillet J-P, Calcagno AM, Varma S, Marino M, Green LJ, Vora MI, et al. Redefining the relevance of established cancer cell lines to the study of mechanisms of clinical anti-cancer drug resistance. *Proc Natl Acad Sci USA.* 2011;108:18708–13.
- Willyard C. The boom in mini stomachs, brains, breasts, kidneys and more. *Nature.* 2015;523:520–2.
- Huch M, Boj SF, Clevers H. Lgr5(+) liver stem cells, hepatic organoids and regenerative medicine. *Regen Med.* 2013;8:385–7.
- Van De Wetering M, Frances HE, Francis JM, Bouanova G, Iorio F, Pronk A, et al. Prospective derivation of a living organoid biobank of colorectal cancer patients. *Cell.* 2015;161:933–45.
- Lee SH, Hu W, Matulay JT, Silva MV, Owczarek TB, Kim K, et al. Tumor evolution and drug response in patient-derived organoid models of bladder cancer. *Cell.* 2018;173:515–28.e517.
- Drost J, Clevers H. Translational applications of adult stem cell-derived organoids. *Development.* 2017;144:968–75.
- Mullenders J, De Jongh E, Brousal A, Roosen M, Blom JP, Begthel H, et al. Mouse and human urothelial cancer organoids: a tool for bladder cancer research. *Proc Natl Acad Sci USA.* 2019;116:4567–74.
- Robertson AG, Kim J, Al-Ahmadi H, Bellmunt J, Guo G, Cherniack AD, et al. Comprehensive molecular characterization of muscle-invasive bladder cancer. *Cell.* 2017;171:540–56.e525.
- Network CGAR. Comprehensive molecular characterization of urothelial bladder carcinoma. *Nature.* 2014;507:315–22.

14. Wolff EM, Liang G, Jones PA. Mechanisms of disease: genetic and epigenetic alterations that drive bladder cancer. *Nat Clin Pract Urol*. 2005;2:502–10.
15. Knowles MA, Hurst CD. Molecular biology of bladder cancer: new insights into pathogenesis and clinical diversity. *Nat Rev Cancer*. 2015;15:25–41.
16. Choi W, Porten S, Kim S, Willis D, Plimack ER, Hoffman-Censits J, et al. Identification of distinct basal and luminal subtypes of muscle-invasive bladder cancer with different sensitivities to frontline chemotherapy. *Cancer Cell*. 2014;25:152–65.
17. Yates DR, Rehman I, Abdo M, Meuth M, Cross SS, Linkens DA, et al. Promoter hypermethylation identifies progression risk in bladder cancer. *Clin Cancer Res*. 2007;13:2046–53.
18. Dudziec E, Miah S, Choudhry HM, Owen HC, Blizzard S, Glover M, et al. Hypermethylation of CpG islands and shores around specific microRNAs and miRNAs is associated with the phenotype and presence of bladder cancer. *Clin Cancer Res*. 2011;17:1287–96.
19. Milne JC, Lambert PD, Schenk S, Carney DP, Smith JJ, Gagne DJ, et al. Small molecule activators of SIRT1 as therapeutics for the treatment of type 2 diabetes. *Nature*. 2007;450:712–6.
20. Wu B, Pan X, Chen X, Chen M, Shi K, Xu J, et al. Epigenetic drug library screening identified an LSD1 inhibitor to target UTX-deficient cells for differentiation therapy. *Signal Transduct Target Ther*. 2019;4:11.
21. Chen J, Zhao L, Peng H, Dai S, Quan Y, Wang M, et al. An organoid-based drug screening identified a menin-MLL inhibitor for endometrial cancer through regulating the HIF pathway. *Cancer Gene Ther*. 2021;28:112–5.
22. Groselj B, Kerr M, Kiltie AE. Radiosensitisation of bladder cancer cells by panobinostat is modulated by Ku80 expression. *Radiother Oncol*. 2013;108:429–33.
23. Yang Z, He L, Lin K, Zhang Y, Deng A, Liang Y, et al. The KMT1A-GATA3-STAT3 circuit is a novel self-renewal signaling of human bladder cancer stem cells. *Clin Cancer Res*. 2017;23:6673–85.
24. Süßmuth SD, Haider S, Landwehrmeyer GB, Farmer R, Frost C, Triepel G, et al. An exploratory double-blind, randomized clinical trial with selisistat, a SirT1 inhibitor, in patients with Huntington's disease. *Br J Clin Pharmacol*. 2015;79:465–76.
25. Van Der Meer AJ, Scicluna BP, Moerland PD, Lin J, Jacobson EW, Vlasuk GP, et al. The selective sirtuin 1 activator SRT2104 reduces endotoxin-induced cytokine release and coagulation activation in humans. *Crit Care Med*. 2015;43:e199–202.
26. Julien C, Tremblay C, Émond V, Lebbadi M, Salem N Jr, Bennett DA, et al. Sirtuin 1 reduction parallels the accumulation of tau in Alzheimer disease. *J Neuropathol Exp Neurol*. 2009;68:48–58.
27. Deng C-X. SIRT1, is it a tumor promoter or tumor suppressor? *Int J Biol Sci*. 2009;5:147.
28. Weinstein JN, Collisson EA, Mills GB, Shaw KRM, Ozenberger BA, Ellrott K, et al. The cancer genome atlas pan-cancer analysis project. *Nat Genet*. 2013;45:1113.
29. Saunders L, Verdin E. Sirtuins: critical regulators at the crossroads between cancer and aging. *Oncogene*. 2007;26:5489–504.
30. Lee JT, Gu W. SIRT1: regulator of p53 deacetylation. *Genes Cancer*. 2013;4:112–7.
31. Li H-T, Duymich CE, Weisenberger DJ, Liang G. Genetic and epigenetic alterations in bladder cancer. *Int Neurotol J*. 2016;20:S84.
32. Faleiro I, Leão R, Binnie A, De Mello RA, Maia A-T, Castelo-Branco P. Epigenetic therapy in urologic cancers: an update on clinical trials. *Oncotarget*. 2017;8:12484.
33. Mitchell SJ, Martin-Montalvo A, Mercken EM, Palacios HH, Ward TM, Abulwerdi G, et al. The SIRT1 activator SRT1720 extends lifespan and improves health of mice fed a standard diet. *Cell Rep*. 2014;6:836–43.
34. Zeng L, Chen R, Liang F, Tsuchiya H, Murai H, Nakahashi T, et al. Silent information regulator, Sirtuin 1, and age-related diseases. *Geriatrics Gerontol Int*. 2009;9:7–15.
35. Carafa V, Altucci L, Nebbioso A. Dual tumor suppressor and tumor promoter action of sirtuins in determining malignant phenotype. *Front Pharmacol*. 2019;10:38.
36. Hu Q, Wang G, Peng J, Qian G, Jiang W, Xie C, et al. Knockdown of SIRT1 suppresses bladder cancer cell proliferation and migration and induces cell cycle arrest and antioxidant response through FOXO3a-mediated pathways. *Biomed Res Int*. 2017;2017:3781904.
37. Chen J, Cao L, Li Z, Li Y. SIRT1 promotes GLUT1 expression and bladder cancer progression via regulation of glucose uptake. *Hum Cell*. 2019;32:193–201.
38. Dioum EM, Chen R, Alexander MS, Zhang Q, Hogg RT, Gerard RD, et al. Regulation of hypoxia-inducible factor 2alpha signaling by the stress-responsive deacetylase sirtuin 1. *Science*. 2009;324:1289–93.
39. Lim JH, Lee YM, Chun YS, Chen J, Kim JE, Park JW. Sirtuin 1 modulates cellular responses to hypoxia by deacetylating hypoxia-inducible factor 1alpha. *Mol Cell*. 2010;38:864–78.
40. Laemmle A, Lechleiter A, Roh V, Schwarz C, Portmann S, Furer C, et al. Inhibition of SIRT1 impairs the accumulation and transcriptional activity of HIF-1α protein under hypoxic conditions. *PLoS One*. 2012;7:e33433.
41. Joo HY, Yun M, Jeong J, Park ER, Shin HJ, Woo SR, et al. SIRT1 deacetylates and stabilizes hypoxia-inducible factor-1α (HIF-1α) via direct interactions during hypoxia. *Biochem Biophys Res Commun*. 2015;462:294–300.
42. Shin DH, Choi YJ, Park JW. SIRT1 and AMPK mediate hypoxia-induced resistance of non-small cell lung cancers to cisplatin and doxorubicin. *Cancer Res*. 2014;74:298–308.
43. Majmundar AJ, Wong WJ, Simon MC. Hypoxia-inducible factors and the response to hypoxic stress. *Mol Cell*. 2010;40:294–309.
44. Chen R, Dioum EM, Hogg RT, Gerard RD, Garcia JA. Hypoxia increases sirtuin 1 expression in a hypoxia-inducible factor-dependent manner. *J Biol Chem*. 2011;286:13869–78.
45. Geng H, Liu Q, Xue C, David LL, Beer TM, Thomas GV, et al. HIF1α protein stability is increased by acetylation at lysine 709. *J Biol Chem*. 2012;287:35496–505.
46. Farghali H, Kemelo MK, Canová NK. SIRT1 modulators in experimentally induced liver injury. *Oxid Med Cell Longev*. 2019;2019:8765954.
47. Sun J, He X, Zhu Y, Ding Z, Dong H, Feng Y, et al. SIRT1 activation disrupts maintenance of myelodysplastic syndrome stem and progenitor cells by restoring TET2 function. *Cell Stem Cell*. 2018;23:355–69.e359.
48. Chini CC, Espindola-Nette JM, Mondal G, Guerrico AM, Nin V, Escande C, et al. SIRT1-activating compounds (STAC) negatively regulate pancreatic cancer cell growth and viability through a SIRT1 lysosomal-dependent pathway. *Clin Cancer Res*. 2016;22:2496–507.
49. Wang Y, Bi Y, Chen X, Li C, Li Y, Zhang Z, et al. Histone deacetylase SIRT1 negatively regulates the differentiation of interleukin-9-producing CD4(+) T cells. *Immunity*. 2016;44:1337–49.
50. Zhao H, Yan C, Hu Y, Mu L, Huang K, Li Q, et al. Sphere-forming assay vs. organoid culture: Determining long-term stemness and the chemoresistant capacity of primary colorectal cancer cells. *Int J Oncol*. 2019;54:893–904.
51. Lahusen TJ, Deng CX. SRT1720 induces lysosomal-dependent cell death of breast cancer cells. *Mol Cancer Ther*. 2015;14:183–92.

ACKNOWLEDGEMENTS

We thank all Chen-Liu laboratory members for their invaluable suggestions and technical support, and Wei team members for patient counseling.

AUTHOR CONTRIBUTIONS

PT, MW, YL, CC, and QW conceived the project, designed experiments, and wrote the paper. PT, MW, YW, JD, JW, LQ, ZB, JZ, and JC performed experiments and analyzed data. PZ, TL, PH, LY, and QG did patient counseling. AZ performed RNA-seq and bioinformatics analysis.

FUNDING

This work was supported by the National Key R&D Program of China (Grant No. 2017YFA0505600), National Natural Science Foundation of China (Grant No. 82002692), 1.3.5. Project for Disciplines of Excellence, West China Hospital, Sichuan University (Grant No. ZYGD18011 and ZY2016104), Post-Doctor Research Project of Sichuan University (Grant No. 2021SCU12016), and Post-Doctor Research Project, West China Hospital, Sichuan University (Grant No. 19HXBH057).

COMPETING INTERESTS

The authors declare no competing interests.

ETHICS APPROVAL AND CONSENT TO PARTICIPATE

The study was approved by the Ethical Research Committee of the West China Hospital (2019-933/2020-330). Written informed consent was obtained from all patients involved. All patients had a confirmed pathologic diagnosis of MIBC and underwent radical cystectomy.

ADDITIONAL INFORMATION

Supplementary information The online version contains supplementary material available at <https://doi.org/10.1038/s41388-021-01999-9>.

Correspondence and requests for materials should be addressed to C.C. or Q.W.

Reprints and permission information is available at <http://www.nature.com/reprints>

Publisher's note Springer Nature remains neutral with regard to jurisdictional claims in published maps and institutional affiliations.